Terra Antartica
2000, **7**(4), 545-552

TERRA ANTARTICA
AN ANTARCTIC EARTH SCIENCE JOURNAL

Erosional History of the Transantarctic Mountains Deduced from Sand Grain Detrital Modes in CRP-2/2A, Victoria Land Basin, Antarctica

J.L. Smellie

British Antarctic Survey, High Cross, Madingley Road, Cambridge CB3 0ET - UK
(j.smellie@bas.ac.uk)

Received 29 July 1999*; accepted in revised form* 22 October 1999

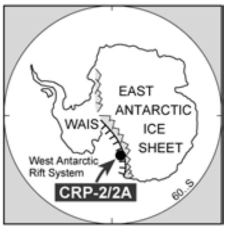

Abstract - Dynamic provenance variations are deduced from sand-grain detrital modes in samples obtained from the CRP-2/2A drillcore. Below an important unconformity at 307 metres below sea floor (mbsf), sand grains in most of the sequence were dominantly derived from Beacon sandstone and Ferrar dolerite sources, although alternating with subordinate thicknesses of strata derived from a predominantly granitoid source (Granite Harbour Intrusive Complex; GHIC). Above the 307 mbsf unconformity, the reverse situation occurs, with most sediments dominantly sourced in the GHIC. Contributions from other sources (*e.g.* Jurassic Kirkpatrick basalt lavas and Proterozoic metamorphic basement) are also persistent but minor. An input of fresh volcanic detritus commenced at 307 mbsf and is ubiquitous in all the younger sediments. At least three (probably four) episodes of volcanism are identified, each lasting 1-2 M.yr in duration. The initial influx at 307 mbsf corresponds to the initiation of the McMurdo Volcanic Group (MVG) at *c.* 25 Ma and is much younger than estimates made previously by other workers for the oldest MVG volcanic activity in the McMurdo Sound region (Eocene?). Simultaneous major changes in the proportion of clast lithologies in CRP-2/2A suggest that the 307 mbsf unconformity is the most important petrological break within the cored sequence. It is speculated that the petrological contrasts across the unconformity are genetically associated with important climatic changes and/or rapid uplift episode(s) in the Transantarctic Mountains.

INTRODUCTION

The Cape Roberts Project is a drilling investigation, using a sea ice platform situated in McMurdo Sound, whose principal objectives are to obtain a fundamental understanding of Cenozoic palaeoclimatic and tectonic history of the Ross Sea region. The background to the project, its detailed aims, methods used and results so far are summarised in Cape Roberts Science Team (1998, 1999). This paper describes the modal petrology of the sand-grade sedimentary rocks in CRP-2/2A. The modal information reveals a pattern of dynamic provenance variations and erosional history that are poorly understood so far but are probably linked to a combination of climatic controls and uplift of the Transantarctic Mountains.

METHODS AND LIMITATIONS

SAMPLE SELECTION AND TREATMENT

Out of 82 samples obtained from the core, 18 were rejected as unsuitable because they were too fine grained or they contained too much muddy matrix. Sixty four samples were selected for modal analysis, representing a mean down-core distribution of one sample every 10 m. However, the sampling interval is irregular and determined by the availability of suitable sandy layers. Some parts of the core are very well represented, with samples every 2 m (*e.g.* 183-201 metres below sea floor (mbsf)). Conversely, the section between 201 and 270 mbsf is poorly sampled, with just 2 modal analyses available. Many of the samples were weakly cemented and friable and they were impregnated in resin prior to slabbing and grinding, followed by acid etching and staining for feldspars (method of Houghton, 1980). Problems of staining for plagioclase in samples from CRP-1 (Smellie, 1998) were not encountered.

DETRITAL MODES, GRAIN TYPES AND COMPOSITIONAL EFFECTS OF GRAIN-SIZE VARIATIONS

300 sand grains were counted in each sample, using the Gazzi-Dickinson method (Dickinson, 1970). Categories of grain types distinguished are those described by Smellie (1998). Note that, in reporting the results and in the discussion that follows, all the detrital modes are recalculated to exclude matrix (<30 _m) and lithic sedimentary grains (Ls). George (1989) and Smellie (1998) also excluded Ls from consideration. It occurs in very minor amounts in all samples - only 6 samples contain have more than 1 % Ls, and it was below determination or absent in 42 samples. Moreover, it is almost entirely of intraformational origin and thus preserves no provenance information. Mean grain size varies widely between samples (from silty very fine sand to medium sand grade). Although the Gazzi-Dickinson method minimises compositional variations caused by a variable grain-size sample set (Ingersoll et al., 1984), the problem is not obviated and variations may be introduced that are independent of provenance. In CRP-1, a grain-size influence on detrital modes was observed and monitored by Smellie (1998) but, because of the random distribution of sample grain sizes down core, the principal effect was increased scatter in the modal diagrams. A

similar compositional dependence on grain size is evident in samples from CRP-2/2A, but its interpretation is not as straightforward as in CRP-1. Although the distribution of samples with the finest grain sizes (silty very fine sand and very fine–fine sand) is more or less uniform throughout the core, there is a clear bimodal distribution for other grain sizes: fine sand samples are restricted to depths above 300 mbsf, whereas all but one of the fine–medium and medium-grained samples occur below that depth (Tab. 1). A grain-size-induced bias to the detrital modes is thus likely. However, monitoring of modal indices that are unaffected by grain size (*e.g*. ratio of rounded to angular quartz) suggests that, as in CRP-1, provenance variations exert a *dominant* influence on the detrital modes. The major effect of grain size variations is probably to increase the data scatter in diagrams and thus mask some of the more subtle provenance-related effects.

RESULTS OF THE DETRITAL MODES

PETROGRAPHY

The rocks are quartzofeldspathic sandstones with the detrital modes summarised in table 1. All grain types occur throughout the section except for unaltered volcanic lithic and glass fragments, which are absent below 310 mbsf. Values for total quartz and feldspar (Q+F) are seldom less than 80% of the mode (only 14 % of samples) and most contain 87 ± 5 % (Fig. 1). The two minerals vary antithetically and quartz is dominant (range: 45->80 %). Plagioclase (both sodic and calcic types) is always the commonest feldspar, with modal values usually twice those for alkali feldspar. Prominent peak abundances for plagioclase (and corresponding low values for quartz) occur at 45-155, 230-300, 470-495 and about 610 mbsf. However, unlike below 300 mbsf, the peaks for plagioclase above 300 mbsf are not reflected by similar peaks for alkali feldspar, suggesting that, above that depth, the feldspar types were derived from at least two sources. Pyroxene is the next most common mineral and abundances vary from 4 to 13 %, with no clear down-core variations.

Minor framework minerals include hornblende, biotite and opaque grains, with a combined mode typically 0.5-4 %. Opaque grains are ubiquitous and modal abundances usually exceed those of hornblende and biotite in the same samples. Above 310 mbsf, the opaque grains are probably mainly volcanic-derived opaque oxides, whereas below 310 mbsf, they include a large proportion of conspicuous carbon grains (Cape Roberts Science Team, 1999). There are also trace amounts of zircon, detrital (non-organic) and bioclastic carbonate, siliceous diatoms and spicules, sphene, garnet, epidote (rarely clinozoisite), kaersutite, aegirine or aegirine-augite, aenigmatite, arfvedsonite and muscovite. Chlorite, actinolite, smectite and prehnite also occur as rare alteration products in hornblende, biotite, plagioclase and pyroxene. Below 417 mbsf, there is significant alteration and replacement of pyroxene by an unidentified mineral (resembling axinite).

Although fragments of relatively coarsely crystalline granitoids and dolerites are ubiquitous, the Gazzi-Dickinson method only counts their constituent sand-size minerals (Dickinson, 1970; Ingersoll et al., 1984). The finer-grained lithic grains (excluding glass) are dominated by unaltered and altered volcanic fragments (Lv). The fresh Lv grains are mainly composed of lathy plagioclase set in brown glass, but minor fragments containing aegirine, colourless glass and/ or alkali feldspar are also present. The altered Lv grains include graphic-textured quartz and feldspar derived from dolerite and granitoids, fine-grained Kirkpatrick basalt (confirmed by XRF analysis of a few texturally-similar clasts; P. Armienti personal communication) and fine crystalline mosaics of alkali-feldspar–quartz probably derived from Lower Palaeozoic felsic dykes (cf. Smellie, 1998). However, because lithic grains of any type are always uncommon (usually < 6 % of the mode), it was not possible to make separate, statistically viable counts for the different Lv types present. Petrographically distinctive lamprophyre grains, encountered rarely in CRP-1 (Smellie, 1998), were not observed but they may have been the source for some of the brown hornblende observed in the core (see also Polozek, this volume). Other types of lithic grains are very uncommon, typically amounting to only << 1 % of the mode. They include polycrystalline quartz (Qp, with > 3 crystals per grain; cf. Basu et al., 1975) and metamorphic rocks composed of finely crystalline quartz-feldspar-mica

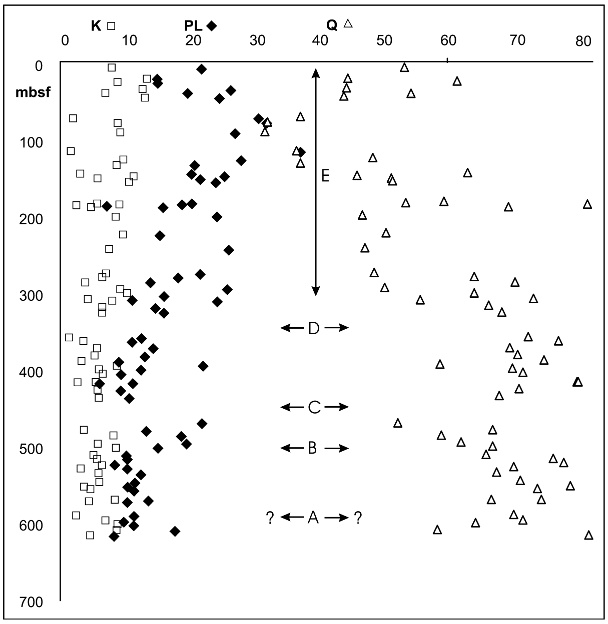

Fig. 1 - Down-core distribution of alkali feldspar (K), plagioclase (PL) and quartz (Q) in CRP-2/2A. Below 300 mbsf, the data for each mineral vary stepwise, and abrupt transitions occur between data "blocks" (indicated by boxes). Positions of the step-like transitions in the data are labelled A-D. Above c. 300 mbsf (metres below sea floor; labelled "E"), the modes are strongly affected by debris derived from coeval volcanism, which affects the absolute values of these indices and any transitions controlled by non-volcanic provenance variations are thus masked. Each box depicted includes most of the samples within selected depth intervals, to illustrate the major modal differences between adjacent depth intervals. Over each interval distinguished, plagioclase and alkali feldspar abundances vary sympathetically, whereas quartz variations are antithetic to the feldspars. By contrast, the prominent lack of a covariation between the feldspar types above 300 mbsf suggests two independent feldspar sources for that depositional period.

Tab. 1 - Detrital modes for sand grains in samples from CRP-2/2A.

sample (mbsf)	Mean grain size	Petrofacies	Qa	Qr	PL	K	PyroxTOT	AmphTOT	Biot	Musc	Qp	Ls	LvMVGbasic	LvMVGevol	LvOther	Lm	Glass, brown	Glass, colourless	Opq	Other	(Matrix%)	Accessory minerals
8,45	VF-F	3	49	2,0	20,3	7,3	7,0	1,0	0,7	0,3	0,3	5,3	2,0	0,0	2,7	0,0	0,3	0,0	1,0	1,0	7,7	Ti-augite, kaersutite, aegirine, gt, diat, spicules, detrital and bioclastic carb, zirc, opq
22,22	VF-F(-M)	4	42	2,3	14,3	13,0	12,0	1,3	1,0	0,0	0,0	1,7	2,7	0,0	3,7	0,0	4,0	1,3	1,0	0,0	4,2	spicules, gt, kaersutite, aegirine
26,77	F	4	56	6,0	14,7	8,7	6,0	0,0	0,0	0,0	0,0	0,0	4,0	0,3	4,3	0,0	0,0	0,3	0,0	0,0	1,0	hyp, Ti-augite, hbl, biot, brown glass, opq
35,84	F(-M)	3	41	3,0	25,7	12,3	12,3	0,3	0,0	0,0	0,0	1,7	0,3	0,0	3,0	0,0	0,0	0,0	0,7	0,0	1,3	hyp, Ti-augite, biot, brown glass
41,81	F	3	52	2,7	19,3	6,7	13,0	0,3	0,0	0,0	0,0	0,3	1,3	0,0	4,0	0,0	0,3	0,0	0,3	0,0	3,8	hyp, biot, gt, detrital carb
46,48	(SILTY-)VF	4	42	1,3	24,3	12,7	10,3	1,0	0,3	0,0	0,0	0,7	1,3	0,0	1,7	0,3	3,0	0,3	0,3	0,0	2,9	hyp, red glass, detrital carb, diat
73,12	F	4	37	0,0	30,3	1,7	10,3	0,7	0,0	0,0	0,0	0,0	1,3	1,0	2,7	0,0	7,3	4,0	1,7	1,7	21,1	aegirine, sphene, detrital carb, diat, epid, spicules, zirc, gt
80,30	silty VF	4	32	0,3	31,7	8,7	9,7	1,0	0,3	0,0	0,0	0,0	1,0	0,3	1,3	0,0	6,0	5,0	2,3	0,7	25,2	aegirine, Ti-augite, red glass, diat, sphene?, spicules
92,20	silty VF	4	31	0,7	26,7	9,0	10,3	0,0	0,0	0,0	0,0	0,0	3,0	0,3	3,7	0,0	6,3	3,7	3,3	2,0	18,0	aegirine, Ti-augite, hbl, biot, musc, red glass, gt, diat, epid?, spicules
117,24	silty VF-F	4	36	0,7	36,9	1,3	6,4	0,3	0,3	0,0	0,0	0,0	2,3	1,7	5,4	0,3	5,4	1,0	2,0	0,0	20,1	Ti-augite, aegirine?, diat, gt, actinolite?
126,53	VF-F	4	46	2,6	27,8	9,6	5,2	0,4	0,0	0,4	0,0	0,0	1,1	0,0	1,1	0,4	1,5	2,6	1,5	0,0	16,7	biot, epid, bioclastic carb, gt, spicules
133,69	VF-F	4	37	0,3	20,3	8,3	10,0	0,3	0,3	0,3	0,0	0,7	3,3	0,0	3,0	1,3	6,7	7,7	0,7	0,0	21,1	red glass, diat, gt
146,23	VF-F	3	60	3,3	19,9	2,7	8,6	0,0	0,0	0,3	0,7	0,3	0,0	0,0	2,3	0,0	0,0	0,0	1,3	0,7	1,6	hbl, biot, brown and colourless glass, sphene/carb
149,73	VF	3	45	0,3	25,0	11,0	11,7	0,3	0,7	0,0	0,0	1,0	0,0	0,0	2,0	0,0	0,7	0,7	1,3	0,0	1,0	aegirine, Ti-augite
152,57	VF-F	3	47	4,1	21,4	5,4	13,6	0,0	1,0	0,0	0,0	0,0	0,3	0,0	2,0	0,0	1,4	0,0	1,7	1,7	2,0	kaersutite, hbl, red glass, detrital carb, epid
155,94	VF(-F)	3	50	1,7	23,7	10,3	9,7	0,3	0,0	0,0	0,0	0,7	0,0	0,0	1,7	0,0	1,3	0,0	1,0	0,0	6,3	Ti-augite, arfveds?, biot, red glass, diat, detrital carb, spicules, zirc?
183,39	silty F	3	50	7,0	19,2	5,2	6,6	0,7	0,4	0,0	0,0	4,1	0,4	0,0	2,6	0,0	0,7	0,0	3,0	0,0	31,4	aegirine, detrital & bioclastic carb, spicules, zirc?
185,06	silty VF-F	3	50	4,0	18,7	9,0	10,3	0,7	0,0	0,0	0,0	0,0	1,0	0,3	1,7	0,3	1,7	1,3	0,7	0,7	13,0	aenig?, biot, detrital & bioclastic carb, diat
186,30	F	3	69	13,0	6,7	2,0	8,7	0,0	0,0	0,0	0,0	0,0	0,0	0,0	0,7	0,0	0,0	0,0	0,0	0,0	0,0	opq, epid
189,30	F	3	66	3,3	15,7	4,3	5,7	0,0	0,0	0,0	0,3	0,7	0,0	0,0	2,7	0,0	0,0	0,3	0,3	0,7	2,9	hbl, brown glass, sphene, gt
200,34	silty VF	4	45	1,3	24,0	8,3	11,0	1,3	1,3	0,7	0,0	0,3	0,0	0,0	0,7	0,0	1,0	2,7	1,0	1,0	18,3	detrital & bioclastic carb, diat
224,46	VF	4	51	0,0	15,0	9,3	8,0	0,7	1,7	0,0	0,3	0,0	1,3	0,0	1,3	0,0	6,0	2,0	3,0	0,7	20,2	aegirine, aenig?, arfveds?, red glass, diat, gt, detrital carb
243,45	VF	4	46	1,3	25,8	7,0	6,0	0,0	0,3	0,0	0,0	0,3	0,0	0,0	0,7	0,3	6,0	2,3	2,3	1,7	17,6	aegirine, hbl, aenig?, orange glass, diat, spicules, detrital carb, sphene?
275,05	F	4	48	0,3	21,3	6,7	8,3	0,3	0,3	0,3	0,0	0,3	1,0	1,0	4,7	0,0	2,0	2,7	1,7	0,7	6,3	aegirine, Ti-augite, epid, detrital carb
280,30	(VF-)F	3	59	5,3	18,0	6,0	4,7	0,3	0,3	0,0	0,0	0,0	0,7	0,0	4,0	0,0	0,3	0,0	1,0	0,3	5,1	aegirine, Ti-augite, colourless glass, epid
287,13	F	3	63	7,6	13,6	3,7	7,3	0,3	0,0	0,0	0,0	0,0	0,3	0,0	3,3	0,0	0,0	0,3	0,3	0,0	0,7	biot, brown glass, gt, diat, zirc, epid
295,11	VF(-F)	3	49	1,0	25,8	9,0	10,7	0,3	0,3	0,0	0,0	0,0	0,0	0,0	3,0	0,0	0,0	0,0	0,3	0,0	9,9	arfveds?, sphene, diat, bioclastic carb
302,65	VF-F	3	50	1,4	12,6	8,0	4,0	0,6	0,0	0,3	0,0	19,7	0,0	0,0	2,6	0,0	0,3	0,0	0,0	0,3	11,2	opq, epid, zirc
308,28	F-M	3	67	6,7	10,7	3,7	9,0	0,0	0,0	0,0	0,0	0,0	0,0	0,0	1,3	0,0	0,0	0,0	1,0	0,7	11,0	hbl, biot, epid, zirc?, detrital carb
310,10	VF	3	56	0,0	24,0	7,7	9,3	0,3	0,3	0,0	0,0	0,0	0,0	0,0	1,3	0,0	0,0	0,0	1,0	0,0	9,6	Ti-augite?, brown glass, gt, sphene?
318,32	VF(-F)	1	65	2,0	14,3	6,0	9,7	0,7	0,3	0,0	0,0	0,0	0,0	0,0	1,7	0,0	0,0	0,0	0,7	0,0	0,3	gt, sphene
326,73	VF(-F)	1	67	2,0	15,7	6,0	5,7	0,0	0,3	0,0	0,0	0,0	0,0	0,0	3,3	0,0	0,0	0,0	0,3	0,0	0,0	hbl
359,30	F-M	2	68	4,3	12,0	1,0	8,0	0,3	0,0	0,0	0,0	0,3	0,0	0,0	3,7	0,0	0,0	0,0	2,0	0,0	23,5	biot, zirc
364,21	M	2	70	7,7	10,7	3,3	6,0	0,0	0,0	0,0	0,0	0,0	0,0	0,0	1,3	0,0	0,0	0,0	1,0	0,0	11,5	gt, sphene?
372,74	VF-M	2	62	8,3	14,0	5,3	8,7	0,3	0,0	0,3	0,3	0,0	0,0	0,0	1,0	0,0	0,0	0,0	0,0	0,0	6,8	biot, opq, gt
381,75	VF-F	2	65	6,1	12,8	4,7	8,1	0,0	0,0	0,0	0,3	0,0	0,0	0,0	2,7	0,0	0,0	0,0	0,0	0,0	24,1	hbl, biot, opq, detrital carb
389,35	F-M	2	66	9,0	8,7	3,0	6,7	1,0	0,0	0,0	0,0	0,0	0,0	0,0	3,0	0,3	0,0	0,0	1,7	0,3	4,2	biot, gt, detrital carb
394,14	VF	2	58	0,7	22,0	8,7	6,0	0,0	0,0	0,0	0,0	0,0	0,0	0,0	0,3	0,0	0,0	0,0	3,7	0,3	8,8	hbl, biot, gt, epid, sphene
398,98	VF-F	2	65	5,3	12,0	5,7	9,7	0,0	0,0	0,0	0,0	0,0	0,0	0,0	2,0	0,0	0,0	0,0	0,3	0,0	0,0	hbl, gt, prehn
404,96	F-M	2	65	7,3	9,0	6,3	5,3	0,0	0,0	0,0	0,7	0,0	0,0	0,0	4,3	0,0	0,0	0,0	0,7	1,7	7,1	hbl, gt, bioclastic carb
416,96	(F-)M	2	74	6,9	10,9	5,1	0,4	0,0	0,0	0,0	0,4	0,0	0,0	0,0	1,8	0,0	0,0	0,0	0,7	0,4	31,7	hbl, chlor, gt, bioclastic & detrital? carb, zirc
417,75	F(-M)	2	67	13,7	5,7	2,3	6,3	0,0	0,3	0,0	0,0	0,0	0,0	0,0	2,7	0,0	0,0	0,0	0,0	2,0	12,8	hbl, chlor, gt, opq, sphene, "axinite", bioclastic? carb
426,94	F-M	2	61	10,3	9,0	5,3	8,3	0,0	0,0	0,0	1,0	0,0	0,0	0,0	4,3	0,0	0,0	0,0	0,7	0,0	0,0	hbl, gt
435,49	M	2	54	14,0	10,3	5,7	11,0	0,0	0,0	0,0	0,0	0,0	0,0	0,0	4,3	0,0	0,0	0,0	0,3	0,0	0,0	hbl, biot, gt
469,93	(VF-)F	1	50	2,4	21,6	10,8	12,2	0,7	0,7	0,0	0,3	0,3	0,0	0,0	1,0	0,0	0,0	0,0	0,0	0,0	45,0	chlor, epid, diat, bioclastic carb, opq
479,11	VF-F	1	66	1,0	13,0	3,3	9,7	0,0	0,0	0,0	0,0	0,0	0,0	0,0	2,7	0,3	0,0	0,0	3,3	0,3	2,6	hbl, chlor, detrital & bioclastic? carb
486,10	VF	1	56	3,0	18,3	8,0	10,7	0,3	0,7	0,0	0,0	0,3	0,0	0,0	2,0	0,0	0,0	0,0	0,7	0,0	2,3	gt, detrital & bioclastic carb
495,10	VF	1	60	2,0	19,3	5,3	9,3	0,0	0,7	0,0	0,0	0,0	0,0	0,0	2,3	0,0	0,0	0,0	0,7	0,0	2,3	hbl, zirc, gt, detrital carb
500,44	VF-F	1	65	2,0	14,7	8,3	4,3	0,3	0,0	0,0	0,0	0,0	0,0	0,0	1,3	0,0	0,0	0,0	3,7	0,0	18,7	biot, "axinite", gt, zirc
511,46	VF(-F)	2	57	4,3	9,0	4,3	4,7	0,0	0,0	0,3	0,0	8,0	0,0	0,0	3,0	0,0	0,0	0,0	9,7	0,0	3,2	hbl, biot, gt
516,38	VF-F	2	73	4,0	10,0	5,3	7,3	0,0	0,0	0,0	0,0	0,0	0,0	0,0	0,3	0,0	0,0	0,0	0,3	0,0	1,3	hbl, biot
522,96	F-M	2	66	12,7	8,0	6,0	4,0	0,3	0,0	0,0	0,7	0,0	0,0	0,0	2,7	0,0	0,0	0,0	0,0	0,0	17,8	biot, "axinite", gt, opq
528,21	M	2	58	13,0	10,0	3,0	10,0	0,0	0,0	0,0	0,0	0,0	0,0	0,0	5,0	0,0	0,0	0,0	1,3	0,0	3,2	smectite, hbl, gt
535,08	M	2	54	13,7	12,0	5,7	10,7	0,0	0,0	0,0	0,0	0,3	0,0	0,0	3,0	0,0	0,0	0,0	0,3	0,3	26,3	biot, gt
545,64	silty VF-F	2	63	8,7	11,0	5,7	8,7	0,0	0,0	0,0	0,0	0,0	0,0	0,0	2,3	0,0	0,0	0,0	0,7	0,0	21,1	hbl
552,62	F(-M)	2	65	14,3	10,0	3,3	4,0	0,0	0,0	0,0	0,0	0,0	0,0	0,0	3,0	0,0	0,0	0,0	0,3	0,0	0,0	gt
556,66	VF-F	2	69	5,3	11,0	4,3	6,7	0,0	0,0	0,0	0,0	0,0	0,0	0,0	3,0	0,0	0,0	0,0	0,7	0,0	19,1	biot, epid, bioclastic carb, gt, spicules
569,60	F-M	2	57	10,0	13,3	8,0	6,3	0,0	0,7	0,3	0,7	0,7	0,0	0,0	2,7	0,7	0,0	0,0	0,0	0,0	25,4	hbl, gt
570,90	M	2	53	21,7	10,0	4,0	6,3	0,3	0,0	0,0	0,0	0,7	0,0	0,0	3,7	0,3	0,0	0,0	0,3	0,0	0,0	actinolite, gt
590,53	(F-)M	2	58	13,0	11,0	2,0	6,4	0,0	0,3	0,0	0,3	0,0	0,0	0,0	9,0	0,3	0,0	0,0	0,0	0,0	4,2	gt
596,25	F(-M)	1	67	4,7	9,3	6,7	0,3	0,0	0,3	0,0	0,0	0,0	0,0	0,0	4,7	0,0	0,0	0,0	0,0	6,7	6,8	hbl, "axinite", opq, epid
601,36	VF-F	1	63	1,7	11,0	8,7	0,0	0,0	0,0	0,0	0,0	0,0	0,0	0,0	2,7	0,0	0,0	0,0	2,3	10,7	18,5	"axinite", hbl, biot, detrital carb, zirc?, sphene, gt
608,72	silty VF	1	58	1,0	17,3	8,3	9,3	0,0	0,3	0,0	0,0	0,0	0,0	0,0	2,0	0,0	0,0	0,0	1,7	2,3	13,3	hbl, detrital carb, gt
615,69	F-M	1	77	5,7	7,7	4,3	0,3	0,0	0,0	0,0	0,3	0,0	0,0	0,0	3,7	0,0	0,0	0,0	0,7	0,7	15,7	"axinite", hbl, biot, gt

Abbreviations: VF - very fine sand; F - fine sand: M - medium sand. Qa - angular quartz; Qr - rounded quartz; PL - plagioclase; K - alkali feldspar; Pyrox - pyroxene; Amph - amphibole; Biot - biotite; Musc - muscovite; Qp - polycrystalline quartz;
Ls - sedimentary lithic grains; Lv - volcanic lithic grains; MVG - McMurdo Volcanic Group; Evol - evolved; Lm - metamorphic lithic grains. mbsf - metres below sea floor.

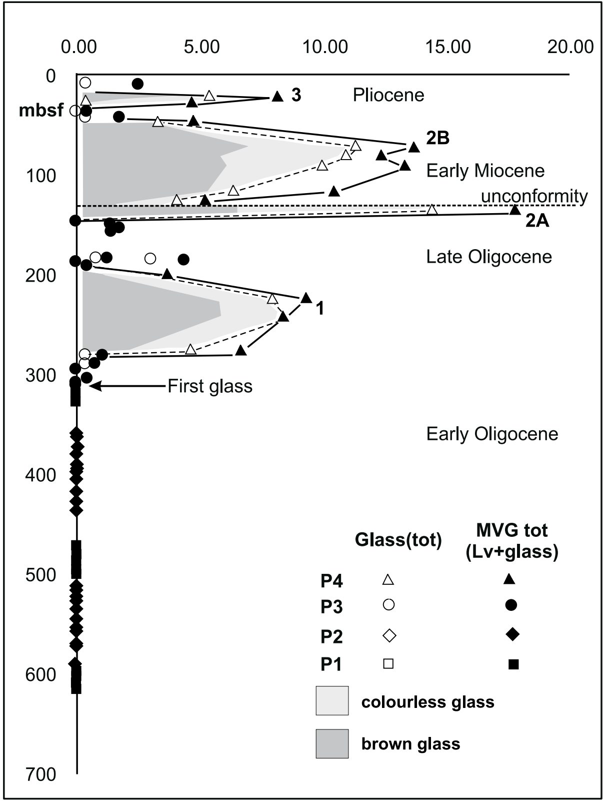

Fig. 2 - Diagram showing the proportion of fresh volcanic detritus in sand-grade samples from CRP-2/2A. Modal indices illustrated are total glass, proportion of brown and colourless glass, and total volcanic detritus (glass plus fresh volcanic lithic grains). All the glass present above 307 mbsf (metres below sea floor) is believed to be derived from the McMurdo Volcanic Group. Prominent volcanic periods are indicated by shading and labelled 1-3. P1-P4 refers to petrofacies 1-4 described in the text.

mosaics that rarely show a tectonite fabric.

Fresh glass fragments (mainly brown and colourless, rarely red) are conspicuous and common above 310 mbsf, with typical modal values of 3-11 % (Fig. 2). The brown glass is poorly to non-vesicular and mainly basaltic, whereas most of the colourless glass is highly vesicular (pumiceous) and has trachytic and phonolitic compositions (P. Armienti, personal communication; see also Armienti et al., 1998, and Smellie, 1998). The glass grains are usually angular but abraded brown and colourless glass are common in a few samples. In almost all cases, modal counts for brown glass exceed those for colourless glass, sometimes by a factor of 4-5 times (Fig. 2). Layers of felsic pumice are also conspicuous above 310 mbsf, particularly at 110-114 and 286 mbsf (Cape Roberts Science Team, 1999).

PETROFACIES

The data can be divided into at least 4 petrofacies, which alternate through the section. Petrofacies 1 and 2 occur below about 300 mbsf, and petrofacies 3 and 4 above that depth. Mean modal values and standard deviations for the principal distinguishing characteristics of the petrofacies are summarised in table 2. A first-order distinction is the restriction to petrofacies 3 and 4 of fresh volcanic lithic and glass fragments and strongly coloured (alkalic) pyroxenes and amphiboles. Petrofacies 4 is rich in fresh volcanic detritus (modal values for Lv+glass ranging between 4 and 18 %; Fig. 2). Petrofacies 1 and 3 are very alike but are easily distinguished by the almost ubiquitous presence of small quantities of fresh Lv and/or glass in petrofacies 3. Petrofacies 2 is characterised particularly by high ratios of rounded to angular quartz (Qr/Qa; Fig. 3) and variable but generally low modal counts for amphibole+mica (often only trace amounts (*i.e.* below determination limit); Tabs. 1 & 2). However, the total counts for Qr are small compared with Qa in all samples, and it is possible that the differences in Qr/Qa ratios are not significant. Conversely, Qr is a simple parameter to measure, unlikely to be confused with any other, and the differences in Qr/Qa ratios between P1 and P2 are large and correlate with several other, unrelated indices (*cf.* Figs. 1 & 3). These observations suggest that the pronounced differences shown by Qr/Qa ratios in the modal data set are reflecting real variations important for petrofacies distinctions.

For many of the modal indices used to distinguish P1 and P2 (*e.g.* Qr/Qa ratios, and modes for quartz, plagioclase, alkali feldspar, amphibole and mica), the transitions between the two petrofacies are distinguished as discrete steps in the data array (*e.g.* Figs. 1 & 3). Although detrital modes involve subjective operator-specific observations, similar sharp changes also occur at the same depths in other CRP-2/2A petrological data sets (*e.g.* sandstone bulk analyses and XRD bulk mineralogy; *cf.* Bellanca et al., this volume, Polozek, this volume, Ehrmann, this volume). However, the P1:P2 transition placed at *c.* 590 mbsf (A in Fig. 1), is relatively poorly defined (mainly by Qr/Qa ratios; *cf.* Figs. 1 & 3) and it is not clearly present in the other petrological data sets. Its status is currently uncertain and requires testing with additional data obtained from greater depths than those reached by CRP-2/2A. By contrast, similar steps are absent from the modal data used to distinguish P3 and P4 (*i.e.* principally total feldspar, plagioclase and glass values) suggesting that transitions between those petrofacies were more gradual (Fig. 2).

Tab. 2 - Summary modal characteristics (mean values and, in parentheses, standard derivations) used to distinguish petrofacies in sand-grade samples in CRP-2/2A.

Petrofacies	No. of samples	Qr/Qa	Glass	Q	F	K	PL	Amph&mica
P4	13	0.03 (0.03)	**7.01 (3.95)**	44 (8)	32.2 (5.4)	8.1 (3.5)	24.1 (6.9)	1.17 (0.99)
P3	17	0.07 (0.05)	**0.58 (0.79)**	59 (11)	26.1 (8.0)	6.9 (3.1)	19.2 (5.4)	0.63 (0.54)
P2	23	**0.15 (0.09)**	**absent**	**73 (5)**	**15.7 (4.3)**	**4.7 (1.8)**	**11.0 (3.0)**	**0.20 (0.10)**
P1	11	0.04 (0.02)	**absent**	66 (8)	21.7 (5.7)	6.9 (2.2)	14.8 (4.3)	0.49 (0.46)

Entries printed in bold are important discriminant characteristics of specific petrofacies.
Abbreviations: Q - quartz (total); F - feldspar (total); K - alkali feldspar; PL - plagioclase; Amph - amphibole; mica - biotite+muscovite.

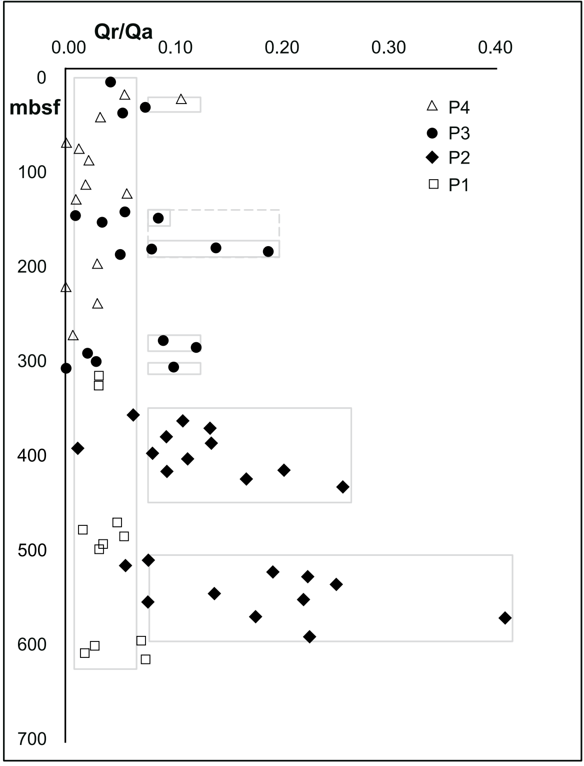

Fig. 3 - Distribution of rounded to angular quartz (Qr/Qa) ratios in CRP-2/2A. High Qr/Qa ratios are characteristic of petrofacies P2, but their recurrence in petrofacies P3 indicates a similar provenance for both petrofacies. P1-4: petrofacies 1-4. mbsf - metres below sea floor.

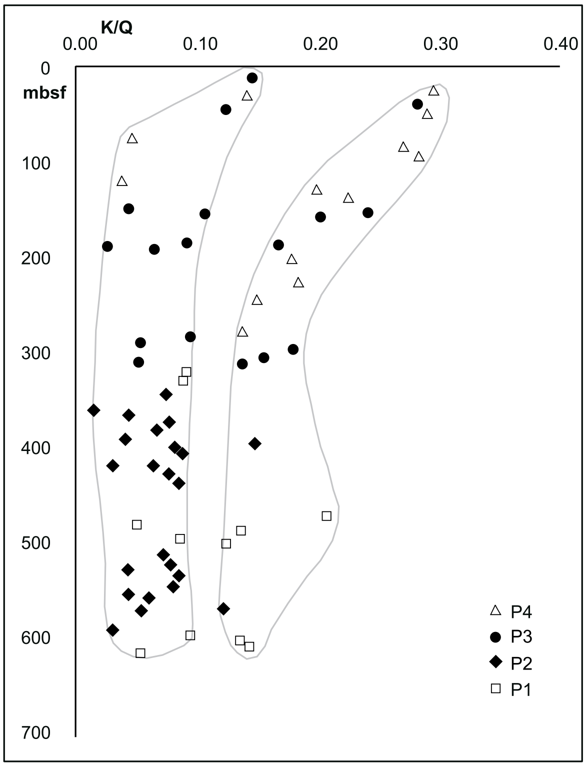

Fig. 4 - Alkali feldspar:quartz (K/Q) ratios in sand-grade samples from CRP-2/2A, illustrating the division of the data into two prominent groups (outlined), reflecting major differences in provenance. Note how almost all of the samples from petrofacies 2 (with high Qr/Qa ratios) fall within the "low-K/Q" group. The group with higher K/Q ratios is dominated by samples with lower Qr/Qa ratios and it also shows a pronounced up-section increase in K/Q values above *c*. 300 mbsf (metres below sea floor).

Another important observation is the distribution of alkali feldspar/quartz and plagioclase/quartz (K/Q, PL/Q) ratios, which clearly divide into two up-core-diverging groups (Fig. 4). There is substantial correspondence in data grouping between the K/Q, PL/Q and Qr/Qa plots, with high Qr/Qa samples having low K/Q and PL/Q ratios and *vice versa*, suggesting a strong provenance control (see below).

DISCUSSION

With the exception of fresh Lv and glass (restricted to P3 and P4), all four petrofacies contain the same grain types. The grain types are also identical to those encountered in CRP-1 and a similar provenance rooted in the Transantarctic Mountains (TAM) is inferred for the entire sample suites in both boreholes. That provenance consisted of coarse-grained plutonic rocks (presumably the Cambro-Ordovician Granite Harbour Intrusive Complex (GHIC)), quartzose sandstones of the Devonian-Triassic Beacon Supergroup, Jurassic Ferrar dolerites and Kirkpatrick basalts, and minor metamorphic rocks (Upper Proterozoic metamorphic basement?; *cf*. Smellie, 1998). The association between glass and strongly coloured amphiboles and pyroxenes (as discrete grains and within Lv fragments) suggests an alkalic volcanic provenance interpreted as the McMurdo Volcanic Group (MVG; *cf*. Armienti et al., 1998). Similar interpretations were reached based on the types of clasts present, and bulk analyses of sandstones and mudrocks (Talarico & Sandroni, 1998; Bellanca et al., this volume; Krissek & Kyle, this volume; Talarico et al., this volume).

Distinctions between the petrofacies are based on the different relative proportions of the grain types (Tab. 2). These indicate differing contributions from the lithologically distinctive units within the TAM. High Qr/Qa ratios can be used to identify unambiguously material derived from the Beacon Supergroup, mainly the Taylor Group (Devonian) in which rounded quartz grains are abundant (*cf*. Korsch, 1974; Barrett et al., 1986; George, 1989; Smellie, 1998). Thus, petrofacies P2, with its distinctive high to very high Qr/Qa ratios (Fig. 3) coupled with a generally lower proportion of basement-derived minerals (*e.g*. amphibole and mica), is clearly identified as having had a dominant source rooted in the Beacon Supergroup. Similarly several samples in P3, with high Qr/Qa ratios, also had a strong Beacon Supergroup influence. However, most samples in P3, and virtually all those in P1 and P4 have low Qr/Qa ratios. Almost all of the low-Qr/Qa samples have relatively high K/Q (and PL/Q) ratios and amphibole and mica contents (Fig. 4) indicating a very different dominant source from P2. K/Q ratios for a variety of granitoid clasts in CRP-1 have mean values about 0.75, whereas values of ≤ 0.11 are more characteristic of Beacon Supergroup sandstones (calculated from data in Korsch, 1974, and Talarico & Sandroni, 1998). Most of the P2 and P3 samples with high Qr/Qa ratios have K/Q ratios between 0.03 and 0.1 (mean 0.07), consistent with a predominantly Beacon Supergroup source, whereas K/Q ratios in low-Qr/Qa samples are higher, mainly 0.12-0.30

(mean 0.15). These ratios are generally too high for a single, Beacon Supergroup source. In figure 4, it is evident that K/Q ratios are relatively constant within the low-K/Q group (mainly 0.03-0.09), rising slightly in only the three youngest samples (0.12-0.14). Similarly, K/Q is also relatively constant within the higher-K/Q group (at *c.* 0.12-0.18) below about 300 mbsf. However, above that depth, K/Q increases and reaches a peak value of 0.30 in the Pliocene sample at 22.22 mbsf. The more rapid rate of increase in K/Q values in the latter group, above *c.* 150 mbsf, may be due to the presence of several unconformities that cut out much of the Miocene, Pliocene and an uncertain proportion of the Quaternary (Cape Roberts Science Team, 1999). However, a dominant contribution from a high-K/Q source is indicated, which is here interpreted to be mainly granitoid basement of the GHIC. The data distribution suggests that the relative contribution from a GHIC source steadily increased in sediments above *c.* 300 mbsf.

During the Oligocene period (below *c.* 300 mbsf), the sediment supply fluctuated between granitoid- and Beacon-dominated, corresponding to petrofacies P1 and P2. The abrupt transitions between P1 and P2 seem to correspond to unconformities, in two instances, but the sample spacing is too wide to be certain. Conversely, a closer sample spacing at the two other P1:P2 transitions suggests that no unconformities are involved, and that the transition may occur *within* sedimentologically-defined Lithological Units.

Detrital input from Ferrar dolerite sources is empirically judged by the proportion of pyroxene present, since most sand-grade pyroxenes were derived from that source (Smellie, 1998). The data scatter is large. Apart from a possible slight increase above 300 mbsf attributed to input of volcanic (MVG) pyroxenes, there are no consistent down-core variations in pyroxene abundances that can be related to other modal indices or to the petrofacies (Tab. 1). Pyroxene abundances in the heavy mineral fraction and determined by bulk mineralogy XRD also show similar down-core abundances (Neumann & Ehrmann, this volume; Polozek, this volume), although a somewhat stepped distribution is suggested by the latter. All of these studies suggest that the Ferrar-derived input was relatively constant throughout the CRP-2/2A sequence. Examination of geological maps of south Victoria Land suggests that the present-day bedrock outcrop is dominated by Ferrar dolerite north of the Mackay Glacier (> *c.* 60 %). The proportion diminishes southwards, from c. 30-40 % between Mackay and Ferrar glaciers, to << 20 % in outcrops south of Ferrar Glacier (McElroy & Rose, 1987; Allibone et al., 1991; Turnbull et al., 1992; Pocknall et al., 1994; Isaac et al., 1996). These visual estimates mask significant lateral and vertical variations. In particular, the proportion of Ferrar dolerite contained in the pre-Beacon basement outcrop is always much lower (seldom exceeding 20 %) than that intruding Beacon strata.

It is possible to test iteratively the relative volumetric inputs from the two provenances using 1) empirical mass balance calculations (*i.e.* assuming a specified contribution (in %) from each source), and 2) calculated mean modal compositions for Beacon sandstones and Ferrar dolerite (data from Korsch, 1974, and Claridge & Campbell, 1984). Using an initial mean value of 50 % for Ferrar dolerite:Beacon strata, the results suggest that the Beacon-dominated sediments (*i.e.* those with high Qr/Qa ratios), whose principal additional provenance should only be Ferrar dolerite, will have mean Q/F ratios *c.* < 2. However, mean ratios measured in CRP-2/2A samples are much higher (nearly 5). To balance the data requires that the provenance was dominantly composed of up to 80 % Beacon strata and *c.* 20 % Ferrar dolerite. Recalculating the proportion of pyroxene using an 80:20 ratio (Beacon:Ferrar) correctly predicts the measured mean modal abundance of that mineral in CRP-2/2A samples (estimated at *c.* 9 %; measured values mainly 6-12 %), giving some confidence in the method. If true, this result indicates that the Oligocene-Miocene sediment supply to the Ross Sea basin was not derived mainly from the Transantarctic Mountains north of the Mackay Glacier (composed of > 60 % Ferrar dolerite). Conversely, the lack of significant down-core variations in pyroxene abundances in CRP-2/2A samples suggests that dolerite/granitoid and dolerite/Beacon proportions were broadly similar in the two terrains, whereas mapping suggests a generally lower proportion of dolerite intruding the granitoid basement. However, the data scatter is large and may mask important variations. Moreover, the extent of the present-day outcrops may not be representative of those in the Oligocene and Miocene and the respective catchment areas during those periods. In particular, the outcrop of pre-Beacon basement may have been smaller and at lower elevations, with Ferrar dolerite (which is probably more common in the upper part of the granitoid basement) better represented.

The problematical antithetic relationship between Qr/Qa and pyroxene/quartz ratios reported for CRP-1 (Smellie, 1998) probably has no provenance significance. The much larger data set now available for CRP-2/2A shows that Qr/Qa ratios are proportional to Q (although the data scatter is large). An antithetic relationship between the ratios is therefore forced by variations in the proportion of the volumetrically dominant and independently-sourced quartz grains.

The principal difference between petrofacies P1 & P2 and P3 & P4 is the presence of MVG detritus in the latter. When the volcanic influence is stripped away, an underlying contribution from granitoid and Beacon provenances essentially indistinguishable from P1 & P2 is revealed. Thus, the volcanic contribution is simply superimposed on a continuing influx of detritus eroded from the TAM. However, a fundamental dichotomy in the detrital modes occurs at about 300 mbsf, and it is also shown simultaneously in the data for clast abundances (Talarico et al., this volume). As an important unconformity is present at 307 mbsf, it is suggested that the dichotomy is genetically associated with the development of that unconformity. Below *c.* 300 mbsf, sedimentation was dominated for long periods alternately by Beacon, then granitoid sources, with Beacon-derived sediments predominant (> 65 % of the section). Above that depth, Beacon-dominated sedimentation affected much thinner sequences (< 20 % of the section) and the bulk of the sedimentation was sourced mainly in granitoids whose influence increased in the younger units (*cf.* Fig. 4). The *simplest* explanation for these observations is that, at *c*. 307 mbsf, corresponding approximately to 25 Ma, the granitoid outcrop became much more extensive, whereas Beacon strata were the dominant outcrop for substantial periods prior to that time. It is possible to depict radically different fluvial transport paths crossing the Beacon and GHIC outcrops (reflecting different TAM gradients and topographies) that could lead to the sediment supply being dominated by either provenance at different times. However, it is much harder to envisage a realistic mechanism whereby the morphological changes required to influence TAM topography could occur so rapidly and so profoundly by sedimentary methods alone. Substantial climatic change(s) and/or rapid uplift of the TAM at *c*. 25 Ma are also likely to be implicated, leading to a lower base level and widespread downcutting into the GHIC, which then became the predominant provenance for the younger sequences.

COEVAL VOLCANIC ACTIVITY

Evidence for alkaline MVG volcanism coeval with sedimentation is restricted to samples above 310 mbsf, particularly in petrofacies P4, in which fresh volcanic grains are characteristic and abundant (Fig. 2). At least three prominent peak modal abundances are evident: 1. Pliocene, 2. Early Miocene–latest Oligocene and 3. Late Oligocene, corresponding approximately to Lithofacies Units 2.2, 4.1-8.2 and 9.3-9.7, respectively. However, the volcanism that commenced in the latest Oligocene is truncated by an unconformity, above which the volcanic input is markedly diminished before rising rapidly to another peak. These observations suggest that there may have been a latest Oligocene episode (episode 2A) followed, probably after a comparatively short time, by Early Miocene volcanism (episode 2B). The Miocene and Oligocene episodes are also associated with several evolved pumice units (Cape Roberts Science Team, 1999). The volcanic periods were substantial, affecting a total thickness of about 190 m of strata. The volcanism was bimodal (basalt–trachyte/phonolite) but, in almost all samples, basaltic compositions were dominant. Volcanic-related modal indices (*e.g*. fresh Lv, glass, plagioclase) have "humped" profiles (Figs 1 & 2), indicating that the volcanism built up and then diminished over (short) periods rather than the stepped profiles and sudden modal changes characteristic of boundaries between petrofacies P1 and P2. ^{40}Ar/^{39}Ar dating of tephra (McIntosh., this volume) indicates that each episode in the Miocene and Oligocene could represent about 1-2 M.yr. of volcanic activity.

Below the 307 mbsf unconformity, only a single grain of glass (brown) was observed (at 310 mbsf). Rare grains of brown glass were also observed in the heavy mineral suite below that depth by Polozek (this volume), but are not yet analysed. However, XRF analyses of some glass-bearing clasts have confirmed a Kirkpatrick basalt provenance (P. Armienti, personal communication). Brown glass is common in Kirkpatrick basalt lavas (Elliot et al., 1995). Fragments of Kirkpatrick basalt lavas were first identified in CRP-1 (Smellie, 1998) and are common as clasts and grains in CRP-2/2A (Talarico et al., this volume, and Smellie, this paper). Minerals associated with alkaline volcanism (*e.g*. coloured pyroxenes, sanidine, anorthoclase) and any obvious alkaline MVG influence on sandstone and mudrock compositions are also absent below 307 mbsf (Bellanca et al., this volume; Krissek & Kyle, this volume). Thus, the apparent absence of MVG-derived debris below 307 mbsf in CRP-2/2A suggests that MVG activity in the McMurdo Sound region commenced at that depth, corresponding to an age of about 25 Ma. Although George (1989) reported that MVG volcanism affected samples right to the base of the CIROS-1 sequence (Eocene? Hannah, 1997), it seems likely that the provenance of the volcanic grains in the lower part of CIROS-1 was misidentified, and they could also have been derived from a Kirkpatrick basalt source.

CONCLUSIONS

Detrital modes of 64 sand-grade samples from the CRP-2/2A drillcore reveal a pattern of changing grain types that indicate dynamic provenance variations over time. Four major petrofacies are distinguished, which alternate up through the section. In the lower half of the section, most of the sediment was dominated by Beacon-derived detritus (petrofacies P2) but it alternates with subordinate sediments formed from a mainly granitoid source (GHIC; petrofacies P1). The pattern of modal variations suggests abrupt transitions between the two petrofacies. In the upper half of the section, the proportion of Beacon detritus diminishes markedly and is replaced by a major input from granitoids. The proportion of granitoid detritus increases up-section, presumably reflecting more extensive exposure than during the previous period. Uplift or important climate change(s), occurring at *c*. 307 mbsf and corresponding approximately to 25 Ma, are likely to have been involved in the change from a provenance composed mainly of Beacon strata with minor granitoids, up to one dominated by more widely exposed granitoids. Ferrar dolerites were also eroded throughout the period represented by CRP-2/2A, and detritus derived from a metamorphic basement and Kirkpatrick basalts is sporadic but persistent, although volumetrically insignificant in the sand population. Fresh volcanic debris is abundant above the 307 mbsf unconformity, particularly in petrofacies P4. At least 3, possibly 4, important compositionally-bimodal volcanic episodes can be distinguished. They include several tephra layers.

ACKNOWLEDGEMENTS

The author is grateful to Ian Turnbull, Jane Forsyth and Duncan Pirrie for their constructive comments on this paper, to Mike Tabecki, once again, for his substantial efforts in making good quality stained thin sections from a wide range of difficult material, and to colleagues at McMurdo and Scott bases and at Cape Roberts for invaluable help and constructive discussions during the course of CRP-2/2A drilling.

REFERENCES

Allibone A.H., Forsyth P.J., Sewell R.J., Turnbull I.M. & Bradshaw M.A., 1991. Geology of the Thundergut area, southern Victoria Land, Antarctica. Scale 1: 50000. *New Zealand Geological Survey Miscellaneous Geological Map 21* (map and notes), Wellington, New Zealand, Department of Scientific and Industrial Research.

Armienti P., Messiga B. & Vannucci, R., 1998. Sand provenance from major and trace element analyses of bulk rock and sand grains. *Terra Antartica*, **5**(3), 589-599.

Barrett P.J., McKelvey B.C. & Walker B.C., 1986. Sand provenance. In: Barrett P.J. (ed.), *Antarctic Cenozoic History from the MSSTS-1 Drillhole, DSIR Bulletin*, **237**, 137-144.

Basu A., Young S.W., Suttner L.J., James W.C. & Mack G.H., 1975. Re-evaluation of the use of undulatory extinction and polycrystallinity in detrital quartz for provenance interpretation. *Jour. of Sedim. Petrol.*, **45**, 873-882.

Cape Roberts Science Team, 1998. Inital Report on CRP-1, Cape Roberts Project, Antarctica. *Terra Antartica*, **5**(1), 187 p.

Cape Roberts Science Team, 1999. Studies from the Cape Roberts Project, Ross Sea, Antarctica. *Terra Antartica*, **6**(1/2), 173 p.

Claridge G.G.C. & Campbell I.B., 1984. Mineral transformation during the weathering of dolerite under cold arid conditions in Antarctica. *New Zealand Journal of Geology and Geophysics*, **27**, 537-545.

Dickinson W.R., 1970. Interpreting detrital modes of graywacke and arkose. *Jour. of Sedim. Petrol.*, **40**, 695-707.

Elliot D.H., Fleming T.H., Haban M.A. & Siders, M.A., 1995. Petrology and mineralogy of the Kirkpatrick Basalt and Ferrar Dolerite, Mesa Range region, North Victoria Land, Antarctica. In: Elliot, D.H. & Blaisdell, G.L. (eds.) *Contributions to Antarctic Research IV. AGU Antarctic Research Series*, **67**, 103-142.

George A., 1989. Sand provenance. In: Barrett P.J. (ed.) *Antarctic Cenozoic History from the CIROS-1 Drillhole, McMurdo Sound, DSIR Bulletin*, **245**, 159-167.

Hannah M.J., 1997. Climate controlled dinoflagellate distribution in Late Eocene/earliest Oligocene strata from the CIROS-1 drillhole. *Terra Antartica*, **4**(2), 73-78.

Houghton H.F., 1980. Refined techniques for staining plagioclase and alkali feldspars in thin section. *Jour. of Sedim Petrol.*, **50**, 629-631.

Ingersoll R.V., Bullard T.F., Ford R.L., Grimm J.P., Pickle J.D. & Sares S.W., 1984. The effect of grain size on detrital modes: a test of the Gazzi-Dickinson point-counting method. *Jour. of Sedim. Petrol.*, **54**, 103-116.

Isaac M.J., Chinn T.J., Edbrooke S.W. & Forsyth P.J., 1996. Geology of the Olympus Range area, southern Victoria Land, Antarctica. Scale 1: 50000. *Institute of Geological & Nuclear Sciences geological map 19*, 1 sheet and 60 p. Institute of Geological & Nuclear Sciences Ltd, Lower Hutt, New Zealand.

Korsch R.J., 1974. Petrographic comparison of the Taylor and Victoria Groups (Devonian to Triassic) in south Victoria Land, Antarctica. *New Zealand Journal of Geology and Geophysics*, **17**, 523-541.

McElroy C.T. & Rose, G., 1987. Geology of the Beacon Heights area, southern Victoria Land, Antarctica. Scale 1: 50000. *New Zealand Geological Survey Miscellaneous Geological Map 15* (map and notes), Wellington, New Zealand, Department of Scientific and Industrial Research.

Pocknall D.T., Chinn T.J., Sykes R. & Skinner D.N.B., 1994. Geology of the Convoy Range area, southern Victoria Land, Antarctica. Scale 1: 50000. *Institute of Geological & Nuclear Sciences geological map 19*, 1 sheet and 36 p. Institute of Geological & Nuclear Sciences Ltd, Lower Hutt, New Zealand.

Smellie J.L., 1998. Sand grain detrital modes in CRP-1: provenance variations and influence of Miocene eruptions on the marine record in the McMurdo Sound region. *Terra Antartica*, **5**(3), 579-587.

Talarico F. & Sandroni S., 1998. Petrography, mineral chemistry and provenance of basement clasts in the CRP-1 drillcore (Victoria Land Basin, Antarctica). *Terra Antartica*, **5**(3), 601-610.

Turnbull I.M., Allibone A.H., Forsyth P.J. & Heron D.W., 1992. Geology of the St Johns Range - Bull Pass area, southern Victoria Land, Antarctica. Scale 1: 50000. *Institute of Geological & Nuclear Sciences geological map 14*, 1 sheet and 52 p. Institute of Geological & Nuclear Sciences Ltd, Lower Hutt, New Zealand.